13.5 g (0.586 mmol) of sodium was added over 30 min. Upon completion the resulting solution was a pale yellow. After evaporation of the ammonia, the salts were filtered under nitrogen through a glass filter and washed repeatedly with petroleum ether. The washings were combined, concentrated, and distilled to yield 91.5 g (95%) of pure hexamethylditin: bp 61 °C (12 torr) [lit.[26] bp 182 °C (756 torr)]; NMR (CCl_4) δ 0.21 (s, ^2J(SnCH) = 48 Hz, ^3J(SnSnH) = 16 Hz, $((CH_3)_3Sn)_2$) [lit.[25] NMR (C_6H_6) δ 0.22 (s, ^2J(SnCH) = 48 Hz, ^3J(SnSnCH) = 16 Hz)].

Trimethyltinsodium. In a typical reaction 0.36 g (15.6 mmol) of finely cut sodium was added to 17 mL of dry THF in a three-neck flask equipped with a Hershberg stirrer and nitrogen gas bubbler. Hexamethylditin, 2.24 g (6.8 mmol), was added and the mixture was stirred at 0 °C for 4 h. The small amount of black precipitate which had formed was allowed to settle; the supernatant was removed and centrifuged in order to remove any additional particles. The concentration of the solution was determined by reaction of a 1-mL aliquot with excess 1-bromobutane which quantitatively yields 1-butyltrimethyltin. The above solution was 0.61 M.

Reaction of Trimethyltinsodium with 1-Bromoadamantane in the Presence of *tert*-Butyl Alcohol. To 0.389 g (1.809 mmol) of 1-bromoadamantane, 0.293 g (1.74 mmol) of dodecane, and 0.485 g (6.54 mmol) of *tert*-butyl alcohol in 1 mL of THF was added 4 mL of a 0.75 M trimethyltinsodium solution at 0 °C. The vial was then cooled to −10 °C for 12 h. GLC analysis yielded 60% unreacted 1-bromoadamantane and 40% adamantane.

Reaction between Trimethyltinsodium and *tert*-Butylamine. To 1 mL of a 0.61 M solution of trimethyltinsodium in THF was added 4.53 mmol of *tert*-butylamine at 0 °C. After 24 h at −10 °C 1.32 mmol of 1-bromobutane was added and the reaction mixture analyzed by GLC indicated the formation of 98% trimethylphenyltin based on initial trimethyltinsodium.

Reaction between Trimethyltinsodium and Dicyclohexylphosphine. To 1 mL 0.47 M trimethyltinsodium solutions in THF at 0 °C were added varying amounts of dicyclohexylphosphine as shown in Table VI. The reaction mixtures were stored at −10 °C until 1-bromobutane was added at various times (ranging from 0 to 1440 min). Analysis by GLC indictaed the formation of 95 to 100% 1-butyltrimethyltin.

Reaction of Trimethyltinsodium with Bromobenzene in the Presence of *tert*-Butylamine. To a solution containing 0.085 g (0.54 mmol) of bromobenzene, 0.145 g (1.98 mmol) of *tert*-butylamine, and 0.145 g (0.40 mmol) of octane (internal standard) in 0.4 mL of THF was added 1.5 mL (0.87 mmol) of trimethyltinsodium at 0 °C. After 5 min the reaction mixture was analyzed by GLC and indicated the formation of 85% benzene and 15% trimethylphenyltin.

Reaction of Trimethyltinsodium with Bromobenzene in the Presence of *tert*-Butyl Alcohol. To a solution containing 0.081 g (0.52 mmol) of bromobenzene, 0.231 g (3.12 mmol) of *tert*-butyl alcohol, and 0.044 g (0.39 mmol) of octane in 0.2 mL of THF was added 1.5 mL (0.87 mmol) of trimethyltinsodium at 0 °C. GLC analysis of the reaction mixture yielded 82% benzene and 11% trimethylphenyltin.

Reaction of Trimethyltinsodium with Bromobenzene in the Presence of Dicyclohexylphosphine. To a solution containing 0.532 mmol of bromobenzene, 0.347 mmol of octane (internal standard), and 0.730 mmol of dicyclohexylphosphine in 0.5 mL of THF was added 1 mL of a 0.55 M trimethyltinsodium solution at 0 °C. After 5 min the solution was analyzed by GLC and indicated the formation of 30% benzene and 69% trimethylphenyltin.

Trapping Studies. The general experimental procedure for trapping studies of the reaction of trimethyltinsodium with alkyl halides with dicyclohexylphosphine and *tert*-butylamine is presented below. Any variations will be described in the appropriate sections.

Reaction of Trimethyltinsodium with 1-Bromoadamantane in the Presence of Dicyclohexylphosphine. Into nitrogen-flushed vial equipped with screw caps with Teflon bodies and valves and a silicone septum was added 0.32 mL of a THF solution at 0 °C of 0.73 M 1-bromoadamantane (0.23 mmol) and 0.57 M dodecane (0.18 mmol) and varying concentrations of DCPH (0.0, 0.107, 0.313, 0.373, 0.692, 1.14, and 2.28 mmol). Trimethyltinsodium 1 mL (0.41 mmol) was then added by syringe and the solution cooled to −10 °C for 12 h. The reaction was generally complete within 4 h. GLC analysis, temperature programmed 100–250 °C, gave the following order of elution: THF, hexamethylditin, adamantane, dodecane (internal standard), 1-bromoadamantane, 1-adamantyltrimethyltin, and DCPH. Quantitative results are presented in Figure 1.

In the Presence of TBA. In a similar experiment, 1 mL of a 0.64 M trimethyltinsodium solution was added to a solution of 0.107 g (0.50 mmol) of 1-bromoadamantane, 0.041 g (0.24 mmol) of dodecane, and 0.142 g (1.94 mmol) of *tert*-butylamine in 0.3 mL of THF at 0 °C, and cooled to −10 °C for 12 h. TBA was eluted prior to THF in the GLC analysis. 1-Adamantyltrimethyltin: NMR (CCl_4) δ 0.05 (s, ^2J(SnCH) = 48/51 Hz, 9 H, $(CH_3)_3Sn$), 1.6–2.0 (m, 15 H, $C_{10}H_{15}$). Similar experiments were conducted with other traps with the results displayed in Table I.

Kinetics. Solutions in THF at 9 °C, 0.04 to 0.07 M in trimethyltinsodium and 0.03 to 0.5 M in bromocyclohexane, were quenched at 30- to 75-s intervals by addition of *n*-butyl bromide, and the resultant solution was analyzed for *n*-butyltrimethyltin. Bimolecular rate constants were then calculated to be 0.16 ± 0.02 M^{-1} s^{-1}. The same reactions conducted in the presence of 0.25 M dicyclohexylphosphine yielded rate constants of 0.18 ± 0.03 M^{-1} s^{-1}.

Acknowledgment. We are grateful to the National Science Foundation for financial support and M & T Chemicals, Inc., and Cincinnati Milacron Chemicals, Inc., for gifts of chemicals.

Electron-Transfer Reactions and Conformational Changes Associated with the Reduction of Bianthrone

Bernard A. Olsen and Dennis H. Evans*

Contribution from the Department of Chemistry, University of Wisconsin–Madison, Madison, Wisconsin 53706. *Received July 28, 1980*

Abstract: The electrochemical reduction of the low-temperature A form of bianthrone (**1A**) at a platinum cathode in DMF proceeds in a two-electron, irreversible reaction, giving the dianion **3B** which is structurally similar to the high-temperature B form of bianthrone (**1B**), having two planar ring systems twisted about the central connecting bond. The overall reduction involves a large structural change. By contrast, **3B** is rapidly and reversibly oxidized to a structurally similar anion radical, **2B**, and then to **1B** which is not stable at room temperature and converts to **1A** as it diffuses away from the electrode. This scheme was confirmed by cyclic voltammetry and transmission-mode spectroelectrochemistry. Rate constants for both the **1A** → **1B** and **1B** → **1A** reactions were determined, and upper limits were put on the rate constants for the direct electrochemical reduction of **1A** to **2B** or **3B**.

In the past few years a number of examples have been found in which different conformations of a molecule undergo oxidation or reduction at an electrode surface at distinctly different potentials. This behavior was first noted in the oxidation of tet-

0002-7863/81/1503-839$01.00/0

raalkyhydrazines,[1] and later an analogous response was obtained for the reduction of 1,2-dibromides.[2] An understanding of the effects of molecular conformation on reactivity is of general interest, so we sought to examine other species for which conformational effects should be detectable.

Bianthrone [10-(10-oxo-9(10*H*)-anthracenylidene)-9(10*H*)-anthracenone, **1**] is an example of a species whose conformations should show markedly different electron-transfer reactivity. It is a thermochromic substance existing in a low-temperature yellow form, **1A**, which predominates at room temperature and a high-

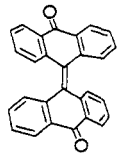

1A

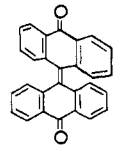

1B

temperature green form, **1B**, which is formed in small amounts when a solution of **1** is heated.[3] **1A** is thought[3] to adopt a doubly folded structure while **1B** has two planar anthrone systems twisted about the connecting double bond by an angle calculated to be about 57°.[4] The anion radical formed by reduction of **1** will probably prefer a twisted configuration, **2B**, and the dianion, **3B**, will definitely exist in a B-type structure, with the dihedral angle between the two planar anthranolate systems probably being close to 90°. Thus the reduction of bianthrone is expected to require a substantial change in structure, **1A** + 2e → **3B**. In this paper we present results of the conformational and electron-transfer reactions among the bianthrone species **1–3** using cyclic voltammetry and transmission-mode spectroelectrochemistry.

The electrochemical behavior of bianthrone in protic media has been reported,[5] and one brief comment on its behavior in *N,N*-dimethylformamide has appeared.[6] Bianthrone is a member of a family of highly hindered species each of which shows interesting electron-transfer reactions. Other representative members include lucigenin (10,10′-dimethyl-9,9′-biacridinium ion),[7] dixanthylene,[8] and dithioxanthylene.[8]

Experimental Section

N,N-Dimethylformamide (DMF, distilled-in-glass grade, Burdick and Jackson) was dried over molecular sieves (Linde Type AW-500). Tetraethylammonium perchlorate (TEAP) was prepared as previously described.[9] Bianthrone (Aldrich Chemical) was used as received; mp 319–320 °C dec. Solutions of bianthrone were protected from exposure to light.

The cell for cyclic voltammetry has been described.[10] The platinum working electrode was the disk portion (0.461 cm²) of a platinum ring-disk electrode (Pine Instrument Co.). An aqueous SCE was used as the reference.

The transmission-mode spectroelectrochemical cell was similar to that of Heineman and Kuwana.[11] The material for the cell body was polyethylene. The platinum optically transparent electrodes (Harrick Scientific) were vapor-deposited platinum films on quartz. The nominal thickness was 100 Å, and the resistance was 20 Ω/sq. The thin-layer spectroelectrochemical cell was similar to that reported by Heineman et al.[12] except that 1000 lines/in. gold minigrid (Buckbee-Mears) was used as the transparent working electrode. The solution path length was 0.016 cm. The silver reference electrode used in the spectroelectrochemical experiments was a silver wire in contact with 0.010 M $AgNO_3$ and 0.10

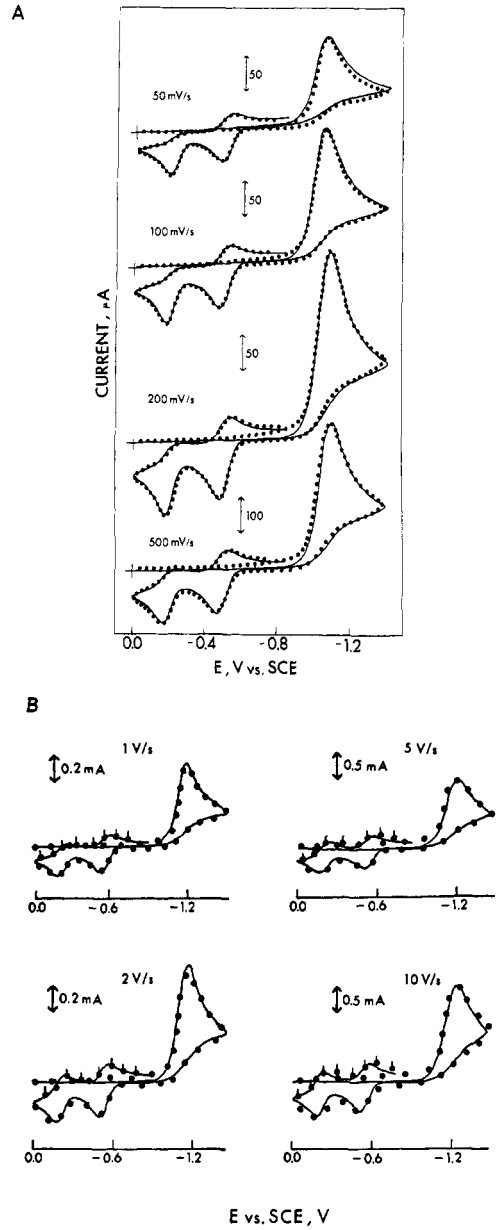

Figure 1. Cyclic voltammetry of bianthrone: 1.12 mM bianthrone in 0.10 M TEAP in DMF; points, experimental; curves, simulations. Simulation parameters: $E_{1B}^0 = -0.195$ V; $E_{2B}^0 = -0.505$ V; $K = 2.2 \times 10^{-3}$; $k_{BA} = 4.7$ s^{-1}; main reduction peak simulated as totally irreversible two-electron process with $\alpha = 0.3$.

Scheme I

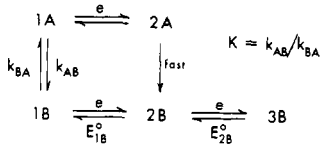

(1) (a) Nelsen, S. F.; Echegoyen, L.; Evans, D. H. *J. Am. Chem. Soc.* **1975**, *97*, 3530–3532. (b) Nelsen, S. F.; Echegoyen, L.; Clennan, E. L.; Evans, D. H.; Corrigan, D. A. *Ibid.* **1977**, *99*, 1130–1134. (c) Nelsen, S. F.; Clennan, E. L.; Evans, D. H. *Ibid.* **1978**, *100*, 4012–4019. (d) Evans, D. H.; Nelsen, S. F. In "Characterization of Solutes in Nonaqueous Solvents"; Mamantov, G., Ed.; Plenum Press: New York, 1977; pp 131–154.

(2) Klein, A. J.; Evans, D. H. *J. Am. Chem. Soc.* **1979**, *101*, 757–758.

(3) For a recent study of bianthrone derivatives with leading references see: Agranat, I.; Tapuhi, Y. *J. Org. Chem.* **1979**, *44*, 1941–1948.

(4) Korenstein, R.; Muszkat, K. A.; Sharafy-Ozeri, S. *J. Am. Chem. Soc.* **1973**, *95*, 6177–6181.

(5) (a) Grabowski, Z. R.; Balasiewicz, M. S. *Trans. Faraday Soc.* **1968**, *64*, 3346–3353. (b) Grabowski, Z. R.; Czochralska, B.; Vincenz-Chodowska, A.; Balasiewicz, M. S. *Discuss. Faraday Soc.* **1968**, *45*, 145–153.

(6) Peover, M. E. *Discuss. Faraday Soc.* **1968**, *45*, 177–178.

(7) (a) Legg, K. D.; Hercules, D. M. *J. Am. Chem. Soc.* **1969**, *91*, 1902–1907. (b) Legg, K. D.; Shive, D. W.; Hercules, D. M. *Anal. Chem.* **1972**, *44*, 1650–1655. (c) Wada, S.; Maeda, K.; Nakada, K. *Nippon Kagaku Kaishi* **1977**, 639–645; (d) Parker, V. D. *Pure Appl. Chem.* **1979**, *51*, 1021–1035.

(8) Kissinger, P. T.; Holt, P. T.; Reilley, C. N. *J. Electroanal. Chem.* **1971**, *33*, 1–12.

(9) Kolthoff, I. M.; Coetzee, J. F. *J. Am. Chem. Soc.* **1957**, *79*, 870–874.

(10) Kinlen, P. J. Ph.D. Thesis, University of Wisconsin, Madison, WI, 1978.

(11) Heineman, W. R.; Kuwana, T. *Anal. Chem.* **1972**, *44*, 1972–1978.

(12) Heineman, W. R.; Norris, B. J.; Goelz, J. F. *Anal. Chem.* **1975**, *47*, 79–84.

M TEAP in DMF (+0.42 V vs. aqueous SCE). Potentials reported are vs. an aqueous SCE.

The cyclic voltammetry instrumentation was the same as that used previously.[13] Spectroelectrochemical instrumentation included a Princeton Applied Research Model 173 potentiostat and a Harrick Scientific Model RSS-B rapid-scan spectrophotometer with a Raytheon 706 computer for instrument control, data acquisition, and data processing. Detailed information about the instrumentation has been presented elsewhere.[14]

The experiments were performed at 21 ± 1 °C.

Results

Cyclic Voltammetry. The electrochemical behavior of bianthrone (**1**) in DMF at the platinum disk electrode is illustrated in Figure 1. A single reduction peak is observed on the first half cycle for the reduction of **1A** to **3B** (see Scheme I), with two oxidation peaks appearing on the second half cycle (**3B** → **2B** and **2B** → **1B**). At rapid scan rates, both the **1B** → **2B** and **2B** → **3B** processes are clearly evident in the third half cycle. The bianthrone formed upon electrochemical oxidation of **3B** is the high-temperature thermochromic form **1B** which converts to **1A** as indicated by the disappearance of the **1B** → **2B** reduction peak at slower scan rates.

Finite difference simulations[15] for Scheme I (curves in Figure 1) were fitted to the experimental data (points) by varying k_{BA}. Best agreement was found for $k_{BA} = 4.7\ s^{-1}$. As expected, the **1B**/**2B** and **2B**/**3B** couples, which involve only minor changes in configuration upon electron transfer, were found to be adequately represented by extremely rapid (electrochemically reversible) electron-transfer reactions. The reduction of **1A** to **3B** was adequately fitted by a totally irreversible two-electron reduction.

These observations are consistent with those of an earlier electrochemical study of bianthrone[6] except for one important feature. Peover[6] found a small oxidation peak at about −0.8 V which he attributed to the oxidation of relatively long-lived **2A** to **1A**. No such peak could be found in the present study. The only way voltammograms like those of Peover could be reproduced was to leave a small concentration of O_2 dissolved in the DMF. The $O_2^{-\cdot} \rightarrow O_2$ peak occurs at the same potential as that reported by Peover for **2A** → **1A**. The peak was absent in completely purged solutions of bianthrone.

The present investigation was prompted in part by the reported[6] stability of **2A**, a species which we felt should convert very rapidly to **2B** which would immediately be reduced to **3B** since the potential is quite negative of the **2B**/**3B** standard potential. An attempt was made to detect **2A** by obtaining voltammograms at rapid scan rates and/or low temperatures. No peak for oxidation of **2A** was ever detected. Failure to detect **2A** at 10 V/s at −45 °C in DMF puts an upper limit of 1.4 ms on its half-life and 10.4 kcal/mol for $\Delta G^{\ddagger}$ (**2A** → **2B**) at −45 °C. It still seems likely that **2A** is an intermediate in the ECE reduction of **1A** to **3B** (Scheme I), but it is too unstable to be detected in our experiments. Its rapid conversion to **2B** causes the first electron transfer (**1A** → **2A**) to become rate limiting which results in a voltammogram with the characteristics of a totally irreversible electrode reaction.[16]

Spectroelectrochemistry. Spectra. The spectra of the stable participants of Scheme I were obtained by thin-layer spectroelectrochemistry and are presented in Figure 2. After the spectrum of starting material **1A** was obtained, the potential was adjusted to −1.4 V vs. an aqueous SCE, resulting in complete conversion to **3B** in about 2 min. Returning the potential to −0.4 V caused the oxidation of **3B** to **2B**, whose spectrum was then obtained. Finally, oxidation at +0.4 V regenerated the original spectrum due to the reaction sequence **2B** → **1B** → **1A**. None of the species shows significant absorbance in the region of the broad absorption band (λ_{max} = 665 nm) observed for the thermochromic form **1B**.[17]

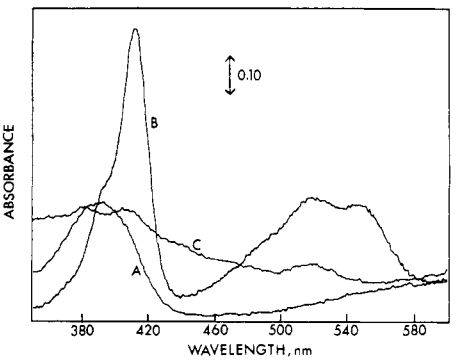

Figure 2. Spectra of bianthrone (**1A**), dianion **3B**, and anion radical **2B**: 1.29 mM bianthrone in thin-layer spectroelectrochemical cell; air reference; 0.10 M TEAP in DMF; spectrum A, initial bianthrone spectrum; spectrum B, spectrum of **3B** obtained after electrolysis at −1.4 V vs. aqueous SCE; spectrum C, spectrum of **2B** obtained after electrolysis at −0.4 V. Spectrum A was quantitatively regenerated after additional electrolysis at +0.4 V.

In the transmission spectroelectrochemical cell which was used for the potential-step experiments, the long solution path length results in a large absorbance by reactant **1A**, ruling out use of wavelengths less than about 440 nm.

Reduction of 1A to 3B. With a 1.27 mM DMF solution of **1A**, the potential of the platinum electrode was stepped to −1.4 V by using the normal (thick layer) transmission cell, and the absorbance due to **3B** at 520 nm was monitored as a function of time for periods ranging from 0.1 to 0.5 s. Each absorbance–time curve was the average of 16 pulses.

For a diffusion-controlled electrode reaction producing an absorbing product, the absorbance is given by[18] eq 1, where ϵ is

$$A = 2\epsilon C^* D^{1/2} t^{1/2} / \pi^{1/2} \quad (1)$$

the molar absorptivity of the product, C^* is the reactant concentration, D is the diffusion coefficient of the reactant, and t is time. Linear plots of A vs. $t^{1/2}$ were obtained, and $\epsilon D^{1/2} = 38.1\ M^{-1}\ s^{-1/2}$ was calculated from the average slope. D was measured under the same conditions by chronoamperometry, and a value of $6.8 \times 10^{-6}\ cm^2/s$ was obtained. Combining these results gives $\epsilon = 1.5 \times 10^4\ M^{-1}\ cm^{-1}$ for **3B** at 520 nm.

The data indicate that the **1A** → **3B** reaction is diffusion controlled, and **3B** is stable for electrolysis time less than about 1 s. At longer times some **3B** disappears (see below).

Formation of 2B by the Sequence 1A → 3B → 2B. Examination of Figure 2 reveals that no wavelength exists where **2B** may be studied without interference by **3B**. However, at 440 nm the ratio of molar absorptivities was favorable, and a double-potential step experiment was performed. A 0.25-s step to −1.4 V produced **3B** from 1.16 mM **1A** as described above. The small ϵ for **3B** resulted in an absorbance at 0.25 s of only 0.006 (25 pulses averaged). The potential was then returned to −0.4 V, causing oxidation to **2B** of the **3B** formed during the first step. The absorbance increased steadily as **3B** was converted to the more strongly absorbing **2B**, reaching a value of 0.012 after 0.25 s at −0.4 V. By use of eq 1, a value of 3500 $M^{-1}\ cm^{-1}$ is calculated for ϵ for **3B** at 440 nm. For a double-potential step experiment where a nonabsorbing reactant (**1A**) is converted during the first step to an absorbing product (**3B**) which is converted during the second step to yet another absorbing species (**2B**), the absorbance–time response for $t > \tau$ is given by[19] eq 2, where τ is the switching time.

$$A = 2C^*(D/\pi)^{1/2}[\epsilon_{2B}\tau^{1/2} + (\epsilon_{2B} - \epsilon_{3B})((t-\tau)^{1/2} - t^{1/2})] \quad (2)$$

The observed absorbance at $t = 0.5$ s combined with ϵ_{3B} just calculated gives an ϵ_{2B} of 9500 $M^{-1}\ cm^{-1}$ at 440 nm. These values

(13) Van Effen, R. M.; Evans, D. H. *J. Electroanal. Chem.* **1979**, *103*, 383–397.
(14) Olsen, B. A. Ph.D. Thesis, University of Wisconsin, Madison, WI, 1979.
(15) Feldberg, S. W. In "Electroanalytical Chemistry"; Bard, A. J., Ed.; Marcel Dekker: New York, 1969; pp 199–296.
(16) Evans, D. H. *J. Phys. Chem.* **1972**, *76*, 1160–1165.
(17) Tapuhi, Y.; Kalisky, O.; Agranat, I. *J. Org. Chem.* **1979**, *44*, 1949–1952.
(18) Strojek, J. W.; Kuwana, T. *J. Electroanal. Chem.* **1968**, *16*, 471–483.
(19) This equation was obtained by a straightforward extension of the method reported: Winograd, N.; Blount, H. N.; Kuwana, T. *J. Phys. Chem.* **1969**, *73*, 3456–3462.

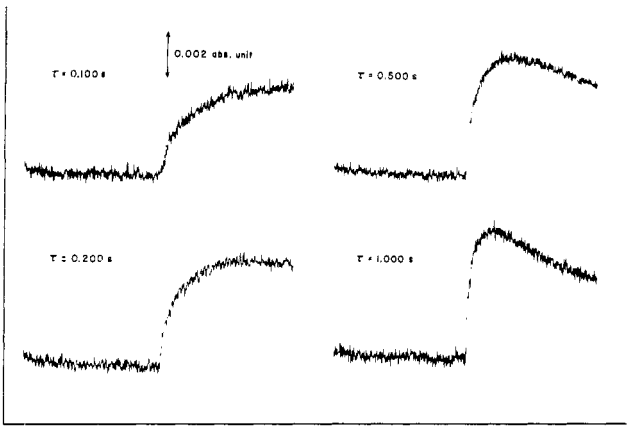

Figure 3. Electrochemical generation and constant-wavelength monitoring of **1B** in double-potential step experiments: 1.00 mM bianthrone in 0.10 M TEAP in DMF. Potential step to −1.3 V vs. aqueous SCE for time τ; return step to +0.4 V; λ = 665 nm; average of 50 pulses at 5-s intervals.

of molar absorptivities are of low precision due to the low measured absorbance, but they are consistent with Figure 2.

Due to overlapping of absorption bands of **3B** and **2B**, transmission spectroelectrochemistry is not well suited for obtaining the spectrum of **2B**. However, that was not the objective because the spectrum was obtained easily by thin-layer spectroelectrochemistry. The intent was to demonstrate that the absorbance at 440 nm changed in a manner consistent with the formation of **2B** in the double-potential step experiment as required by Scheme I.

Formation of 1B by the Sequence 1A → 3B → 1B. The detection of **1B** by spectroelectrochemistry is facilitated by the fact that its 665-nm absorption band is well separated from regions where the reactant and other products absorb. **1B** is formed (rather than **1A**) upon oxidation of **3B** because electron transfer among the structurally similar B configurations is rapid. However, **1B** formed in this manner is far removed from conformational equilibrium and will convert to **1A** as it diffuses away from the electrode. Spectroelectrochemistry should permit quantitative monitoring of the rate of the **1B** → **1A** reaction.

Double-potential step data are presented in Figure 3. During the first step (−1.3 V) **1A** is converted to **3B**, and during the second (+0.4 V) **3B** is oxidized to **1B**. Since neither **1A** nor **3B** absorbs significantly at 665 nm, the absorbance is about zero until $t > \tau$. For small τ the absorbance due to **1B** increases as though **1B** were stable, but as τ is lengthened, a characteristic maximum is observed in the absorbance–time curve due to the relaxation of **1B** to nonabsorbing **1A**. As expected, the absorption band for **1B** (λ_{max} = 665 nm) could be detected by obtaining rapid-scan spectra at t = 1.00 s (1.06 mM **1A**, τ = 0.5 s, average of 50 pulses).

For quantitative analysis of the data, the absorbance at $t = 2\tau$ was measured and compared to theoretical predictions. Theoretical working curves were generated by digital simulation[15] and are displayed (Figure 4) as plots of normalized absorbance, A_N, vs. log $k_{BA}\tau$. A separate curve is obtained for each value of the equilibrium constant, K (Scheme I). The normalized absorbance is the ratio of the observed absorbance at $t = 2\tau$ to the value which would have been observed[19] had **1B** been stable, $0.661\epsilon_{1B}C^*(D\tau)^{1/2}$.

An important consideration in development of the theory for spectroelectrochemistry (as well as for cyclic voltammetry as in Figure 1) is the recognition that during the second step the **1B** diffusing away from the electrode will react with **3B** diffusing toward the electrode (eq 3). The equilibrium constant for this

$$3B + 1B \rightleftharpoons 2B \quad (3)$$

reproportionation reaction can be calculated from the formal potentials of the **1B**/**2B** and **2B**/**3B** couples (Figure 1) to be 9.3 × 10^4, indicating that the radical anion **2B** is favored. Furthermore, this reaction is expected to be very fast so it was assumed to be at equilibrium in all simulations. Loss of **1B** through reproportionation explains why A_N approaches about 0.5 rather than unity at small $k_{BA}\tau$. Measured values of the absorbance at $t = 2\tau$ were used to calculate A_N which in turn yielded $k_{BA}\tau$ by reference to the working curve. Results are summarized in Table I.

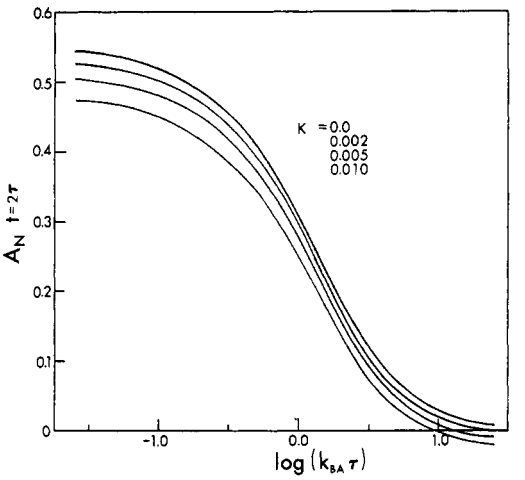

Figure 4. Spectroelectrochemical working curves for double-potential step experiment: K and k_{BA} are defined in Scheme II; τ is the duration of the first step; A_N is the normalized absorbance measured at $t = 2\tau$ (see text).

Table I. Determination of the Rate Constant for Conversion of **1B** to **1A**[a]

bianthrone concn, mM	τ, s	10^3A ($t = 2\tau$)	A_N[b]	k_{BA}, s^{-1} [c]
1.00	0.100	3.40	0.402	4.4
	0.200	3.75	0.314	4.4
	0.300	3.65	0.249	4.2
	0.400	3.35	0.198	4.2
	0.500	3.60	0.191	3.6
	0.600	3.30	0.159	3.6
	0.750	3.05	0.132	3.5
	1.000	3.10	0.116	3.0
1.25	0.500	4.40	0.186	3.7
	0.750	4.15	0.143	3.3
	1.000	3.80	0.114	3.0
1.40	0.500	5.25	0.198	3.5
	0.750	4.60	0.142	3.3

[a] Measured by a double-potential step experiment in 0.10 M TEAP in DMF. See Figure 3 for other conditions. [b] Normalized absorbance. See text for definition. [c] Average value 3.7 ± 0.5 s^{-1}.

A value of 1.55 × 10^4 M^{-1} cm^{-1} was assumed for ϵ_{1B} in the calculation of A_N. This number is based on photochromic studies of bianthrone[20] and has been employed by others.[17] In principle, a value of ϵ_{1B} could be determined from the observed absorbance–time response at low τ. In fact, limited potentiostat/cell response times prevent accurate measurements, but the data at τ = 0.02 s were consistent with ϵ_{1B} = 1.55 × 10^4 M^{-1} cm^{-1}.

The equilibrium constant K, which was needed to select the proper working curve in Figure 4, was obtained by measuring the absorbance of a solution containing **1B** in equilibrium with a known concentration of **1A**. The value of ϵ_{1B} discussed above was used, and the result was K = 2.2 × 10^{-3}.

Open-Circuit Experiments. When **3B** is formed by reduction of **1A** at −1.4 V, the **3B** diffusing away from the electrode will encounter **1A** diffusing to the electrode. These species are capable of reacting with one another as may be seen by calculation of the equilibrium constant for reaction 5 from the known constants for

$$1A \underset{k_{BA}}{\overset{k_{AB}}{\rightleftharpoons}} 1B \quad K = 2.2 \times 10^{-3} \quad (4)$$

(20) Bercovici, T.; Korenstein, R.; Muszkat, K. A.; Fischer, E. *Pure Appl. Chem.* **1970**, *24*, 531–565.

$$\mathbf{1B} + \mathbf{3B} \rightleftharpoons 2\ \mathbf{2B} \quad K_3 = 9.3 \times 10^4 \tag{3}$$

$$\mathbf{1A} + \mathbf{3B} \rightleftharpoons 2\ \mathbf{2B} \quad K_5 = 2.0 \times 10^2 \tag{5}$$

eq 3 and 4. Reaction 5 is assumed to proceed via reaction 4 (rate determining) followed by reaction 3 (fast) in which case its apparent rate constant will be fairly small and equal to k_{AB} ($k_{AB} = k_{BA}K \simeq 10^{-2}$ s^{-1}). As indicated earlier, spectroelectrochemical monitoring of **3B** shows no loss for potential steps of less than 1-s duration. Slower experiments were performed to obtain a rate of disappearance of **3B** which would represent a direct measure of k_{AB}.

The effect is seen most dramatically in open-circuit experiments. **3B** is generated at −1.4 V for a period of time. The cell is then disconnected ("open circuit") so that no electrode reactions can occur, and the absorbance of **3B** is monitored as a function of time. Of course, the absorbance would remain constant if **3B** were stable. Its decrease with time (Figure 5) is caused by the reaction of **3B** with **1A** in the diffusion layer. Digital simulations (points in Figure 5) can be fitted to experiment by using $k_{AB} = 8.1 \times 10^{-3}$ s^{-1}. The data in Figure 5 were obtained at 560 nm where $\epsilon_{3B} > 2\epsilon_{2B}$, so reaction 5 causes a decrease in absorbance. At 480 nm, $\epsilon_{3B} < 2\epsilon_{2B}$ (cf. Figure 2), so the absorbance was found to increase as reaction 5 proceeded. These data were also in excellent agreement with simulations based on $k_{AB} = 8.1 \times 10^{-3}$ s^{-1}.

By judicious choice of the electrochemical experiment and species to be monitored, both the forward and reverse rates of the **1A**/**1B** interconversion have been measured by spectroelectrochemistry.

Discussion

The electron-transfer reactions and conformational changes involving bianthrone in DMF may be quantitatively described by Scheme I with appropriate inclusion of the reproportionation reaction 3. It was found that the structurally similar species **1B**, **2B**, and **3B** are interconverted by very rapid electron-transfer reactions both at the electrode surface and in the solution near the electrode.

By contrast, the reduction of **1A** to **3B** was totally irreversible under all conditions studied. This reaction necessarily involves large structural changes, twisting about the central bond, and flattening of the ring systems. Though we prefer the reduction sequence **1A** → **2A** → **2B** → **3B**, the data do not permit the exclusion of other irreversible two-electron reductions such as the direct reduction of **1A** to **2B** (with the associated large structural change) followed by very rapid reduction of **2B** to **3B**. If **2A** is in fact an intermediate, its lifetime is too short to be detected in our experiments.

It is interesting to examine the kinetic consequences of the structural changes involved in these reduction reactions. The standard potentials for the couples involving the B species were obtained by cyclic voltammetry. These may be combined with K to calculate the standard potentials for two other possible electrode reactions (Table II). Note that both the reduction of **1A** to **2B** and that of **1A** to **3B** are thermodynamically possible for potentials more negative than about −0.4 V vs. SCE. The fact that no reduction of **1A** occurs between −0.4 V and the main reduction peak at −1.0 V (Figure 1) provides a vivid demonstration of the inherent slowness of these electron-transfer reactions, each of which involve electron transfer with simultaneous change in conformation from the A form to the B form.

An upper limit for the standard heterogeneous electron-transfer rate constants can be calculated (Table II) from theory for the position of irreversible cyclic voltammetric peaks[21] and the observation that no peak for **1A** reduction is observed at potentials as negative as −0.8 V at 50 mV/s (Figure 1); i.e., the hypothetical peak potential for a process involving these reactions must be more negative than −0.8 V. The fact that $k_s < 8 \times 10^{-7}$ cm/s for the **1A**/**2B** couple leads to a free energy of activation at 21 °C of >13 kcal/mol when calculated in the manner used by Hale.[22] These calculations illustrate the very substantial barrier which exists for the direct reduction of **1A** to **2B**.

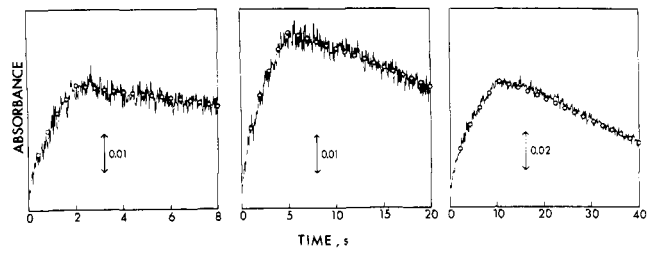

Figure 5. Potential step–open circuit experiments: 1.12 mM bianthrone in 0.10 M TEAP in DMF; potential step to −1.4 V vs. aqueous SCE for 2, 5, and 10 s, respectively; λ = 560 nm; the points represent simulation according to Scheme II with $K = 2.2 \times 10^{-3}$ and $k_{AB} = 8.1 \times 10^{-3}$ s^{-1}; absorbance is due mainly to **3B**; $\epsilon_{3B}/\epsilon_{2B} = 10$.

Table II

couple	E^0, V (vs. SCE)	k_s, cm/s
1B + e ⇌ **2B**	−0.195	*a*
2B + e ⇌ **3B**	−0.505	*a*
1A + e ⇌ **2B**	−0.350	$<8 \times 10^{-7}$ *b*
1A + 2e ⇌ **3B**	−0.428	$<3 \times 10^{-9}$ *b*

[a] The reactions appear reversible at scan rates as large as 50 V/s; k_s exceeds 0.1 cm/s. [b] Calculated (see text) by assuming $\alpha = 0.5$.

As stated earlier, the data do not provide a determination of the mechanism which is actually operative at the main reduction peak of **1A**. The reaction could proceed via the reduction of **1A** to **2B** in the first step, but we prefer the notion that the potential reaches the neighborhood of the standard potential for the facile **1A** → **2A** process and that **2A** rapidly twists to **2B** (Scheme I).

There is another pathway by which **1A** could be reduced, viz., the prior conversion of **1A** to **1B** followed by rapid reduction of **1B** to **2B** and thence to **3B** (Scheme I). From the values of K and k_{AB} measured in this work it can be shown that scan rates less than 10^{-5} V/s would be required to see appreciable currents for such a CE mechanism.[21] Thus, it is not expected that this mechanism would be important at room temperature. However, at elevated temperatures this route becomes more important, and small peaks for **1B** → **2B** and **2B** → **3B** were then seen on the first scan in the negative direction.

The oxidation of **3B** does not proceed directly to the thermodynamically favored **1A**. Instead, the oxidation proceeds along the kinetically favored route via electron transfers within the structurally similar family, **3B**, **2B**, and **1B**. (The relatively small changes in dihedral angle which accompany oxidation and reduction in this series do not contribute enough to the activation energy to affect the results on the time scale of cyclic voltammetry.) The **1B** formed in this manner was found to have the same absorption spectrum as the thermochromic form, confirming that these species are identical.

The bianthrone system provides a rather dramatic example of the effects of molecular conformation on the thermodynamics and kinetics of electron-transfer reactions.

Acknowledgment. Support for this research by the National Science Foundation (Grant CHE78-08727) is gratefully acknowledged. We thank Patricia A. Bitnar for the low-temperature measurements.

(21) Nicholson, R. S.; Shain, I. *Anal. Chem.* **1964**, *36*, 706–723.

(22) Hale, J. M. In "Reactions of Molecules at Electrodes"; Hush, N. S., Ed.; Wiley-Interscience: New York, 1971; pp 229–257.